Optical Kerr Spatiotemporal Dark-Lump Dynamics of Hydrodynamic Origin

Fabio Baronio,[1,*] Stefan Wabnitz,[1] and Yuji Kodama[2,†]
[1]INO CNR and Dipartimento di Ingegneria dell'Informazione, Università di Brescia, Via Branze 38, 25123 Brescia, Italy
[2]Department of Mathematics, Ohio State University, Columbus, Ohio 43210, USA
(Received 26 February 2016; published 27 April 2016)

There is considerable fundamental and applicative interest in obtaining nondiffractive and nondispersive spatiotemporal localized wave packets propagating in optical cubic nonlinear or Kerr media. Here, we analytically predict the existence of a novel family of spatiotemporal dark lump solitary wave solutions of the $(2+1)$D nonlinear Schrödinger equation. Dark lumps represent multidimensional holes of light on a continuous wave background. We analytically derive the dark lumps from the hydrodynamic exact soliton solutions of the $(2+1)$D shallow water Kadomtsev-Petviashvili model, inheriting their complex interaction properties. This finding opens a novel path for the excitation and control of optical spatiotemporal waveforms of hydrodynamic footprint and multidimensional optical extreme wave phenomena.

DOI: 10.1103/PhysRevLett.116.173901

Introduction.—The propagation of intense, ultrashort pulses of electromagnetic radiation in a nonlinear medium is a multidimensional phenomenon, leading to complex spatiotemporal behavior. Pulse dynamics is influenced by the interplay of various physical mechanisms: the most important among them being diffraction, material dispersion, and nonlinear response [1]. Motivated by the strong applicative interest in the generation of high-intensity femtosecond pulses, a significant research activity on spatiotemporal light pulse propagation has been carried out over the past decades. Since the 1990s, theoretical and experimental studies of the self-focusing behavior of intense ultrashort pulses [2–12] have indicated that spatial and temporal degrees of freedom cannot be treated separately. When the three length scales naturally associated with diffraction, dispersion, and nonlinearity become comparable, the most intriguing consequence of space-time coupling is the possibility to form a nondiffractive and nondispersive localized wave packet, namely, a spatiotemporal soliton or light bullet [2]. A strict constraint for the formation of light bullets is that the nonlinear phase changes counteract both the linear wave front curvature and the dispersion-induced chirp, thus leading to space-time focusing [7,9]. Vice versa, normal dispersion rules out the possibility to generate bullet-type spatiotemporal localized wave packets. In this regime, qualitatively different behaviors such as temporal splitting and spectral breaking have been observed [3–6]. In the 2000s, theoretical and experimental studies have demonstrated that nondiffractive and nondispersive localized wave packets also exist within the normal dispersion regime, in the form of the so-called nonlinear X waves, or X-wave solitons [13–15].

Defeating the natural spatiotemporal spreading of wave packets is a challenging and universal task, appearing in any physical context that involves wave propagation phenomena. Ideal particlelike behavior of wave packets is demanded in a variety of applications, such as: microscopy, tomography, laser-induced particle acceleration, ultrasound medical diagnostics, Bose-Einstein condensation, volume optical-data storage, optical interconnects, and those encompassing long-distance or high-resolution signal transmission.

In this Letter, we contribute to the field of nondiffractive and nondispersive spatiotemporal localized wave packets in cubic nonlinear (or Kerr) optical media by predicting the existence and the interactions of dark lump solitary wave solutions of the $(2+1)$D nonlinear Schrödinger equation (NLSE). The key point of our approach consists in that we are able to derive the conditions for optical dark lump solitary waves existence and analytically describe their shape and interactions from the exact soliton solutions of the $(2+1)$D Kadomtsev-Petviashvili (KP) equation [16]. In hydrodynamics, the KP equation describes weakly dispersive and small amplitude water wave propagation in a $(2+1)$D framework, in the so-called shallow water regime (see, e.g., [17–20]). Our results recall and extend the connection between nonlinear wave propagation in optics and hydrodynamics, that was established in the 1990s to describe optical instabilities, dark stripe, and vortex solitons in Kerr media [21–26].

Our treatment below goes as follows. We give first the essential transformations that permit us to construct dark solitary waves of the optical $(2+1)$D NLSE, starting from exact multi-lump solutions of the KP-I equation. We consider the propagation of dark-lump solitary waves in the anomalous dispersion and self-defocusing regime. Then, we highlight complex dark lumps' interactions of the $(2+1)$D NLSE, that surprisingly mimic the behavior of multilump solutions of the KP-I equation. To conclude, we briefly discuss the conditions for the experimental observation of dark lumps in nonlinear optics.

Optical NLSE solitary waves of hydrodynamic KP origin.—The dimensionless time-dependent paraxial wave equation in cubic Kerr media in the presence of group-velocity dispersion and limiting diffraction to one dimension reads as [13]:

$$iu_z + \frac{\alpha}{2}u_{tt} + \frac{\beta}{2}u_{yy} + \gamma|u|^2 u = 0, \tag{1}$$

where $u(t, y, z)$ represents the complex wave envelope; t, y represent temporal and spatial transverse coordinates, respectively; and z is the longitudinal propagation coordinate. Each subscripted variable in Eq. (1) stands for partial differentiation. $\alpha, \beta > 0, \gamma$ are real constants that represent the effect of dispersion, diffraction, and Kerr nonlinearity, respectively. Of course, Eq. (1) may also describe $(2+1)$D spatial dynamics in cubic Kerr media, neglecting group-velocity dispersion; in this case, t, y represent the spatial transverse coordinates, and z the longitudinal propagation coordinate.

Writing $u = \sqrt{\rho}\exp(i\theta)$ and substituting in Eq. (1), we obtain for the imaginary and real parts of the field the following system of equations for (ρ, θ),

$$\begin{aligned} &\rho_z + \alpha(\rho\theta_t)_t + \beta(\rho\theta_y)_y = 0, \\ &\theta_z - \gamma\rho + \frac{\alpha}{2}\left(\theta_t^2 + \frac{1}{4\rho^2}\rho_t^2 - \frac{1}{2\rho}\rho_{tt}\right) \\ &\quad + \frac{\beta}{2}\left(\theta_y^2 + \frac{1}{4\rho^2}\rho_y^2 - \frac{1}{2\rho}\rho_{yy}\right) = 0. \end{aligned} \tag{2}$$

Let us consider now small corrections to the stationary continuous wave (cw) background solutions of Eqs. (2) and set

$$\rho = \rho_0 + \eta, \qquad \theta = \gamma\rho_0 z + \phi, \tag{3}$$

with constant ρ_0. With a small positive parameter $0 < \epsilon \ll 1$, we assume the following scaling $\eta \sim \phi_z \sim \phi_t \sim \mathcal{O}(\epsilon)$, $\partial_t \sim \partial_z \sim \mathcal{O}(\epsilon^{1/2})$, $\partial_y \sim \mathcal{O}(\epsilon)$. That is, we assume a weak nonlinearity, weak diffraction, and slow modulation of cw wave. Then, we obtain from Eqs. (2)

$$\begin{aligned} &\eta_z + \rho_0(\alpha\phi_{tt} + \beta\phi_{yy}) + \alpha(\eta\phi_t)_t = \mathcal{O}(\epsilon^{7/2}), \\ &\phi_z - \gamma\eta + \frac{\alpha}{2}\left(\phi_t^2 - \frac{1}{2\rho_0}\eta_{tt}\right) = \mathcal{O}(\epsilon^3). \end{aligned} \tag{4}$$

Introducing the coordinates $\tau = t - c_0 z$, $\upsilon = y$, $\varsigma = z$ ($c_0 = \sqrt{-\gamma\alpha\rho_0}$) and noting that $\partial_\varsigma \sim \mathcal{O}(\epsilon^{3/2})$, from Eqs. (4), we have

$$\begin{aligned} &-c_0\eta_\tau + \eta_\varsigma + \rho_0\alpha\phi_{\tau\tau} + \rho_0\beta\phi_{\upsilon\upsilon} + \alpha(\eta\phi_\tau)_\tau = \mathcal{O}(\epsilon^{7/2}) \\ &-c_0\phi_\tau + \phi_\varsigma - \gamma\eta + \frac{\alpha}{2}\left(\phi_\tau^2 - \frac{1}{2\rho_0}\eta_{\tau\tau}\right) = \mathcal{O}(\epsilon^3). \end{aligned} \tag{5}$$

From the second of Eqs. (5), we obtain $\eta = -(c_0/\gamma)\phi_\tau + $ *(higher order terms)*; iterating to find the higher order terms, we obtain

$$\eta = \frac{1}{\gamma}\left(-c_0\phi_\tau + \phi_\varsigma + \frac{\alpha}{2}\phi_\tau^2 - \frac{\alpha^2}{4c_0}\phi_{\tau\tau\tau}\right) + \mathcal{O}(\epsilon^3). \tag{6}$$

By inserting (6) in the first of Eqs. (5), we have

$$\phi_{\tau\varsigma} + \frac{3\alpha}{4}(\phi_\tau^2)_\tau - \frac{\alpha^2}{8c_0}\phi_{\tau\tau\tau\tau} + \frac{c_0\beta}{2\alpha}\phi_{\upsilon\upsilon} = \mathcal{O}(\epsilon^3). \tag{7}$$

Equation (7) is known as the potential KP equation [19]. In fact, from Eq. (7), we obtain the evolution equation for η, namely, we have the KP equation at the leading order,

$$\left(-\eta_\varsigma + \frac{3\alpha\gamma}{2c_0}\eta\eta_\tau + \frac{\alpha^2}{8c_0}\eta_{\tau\tau\tau}\right)_\tau - \frac{c_0\beta}{2\alpha}\eta_{\upsilon\upsilon} = 0. \tag{8}$$

Notice that, in the case $\alpha > 0$, $\beta > 0$, $\gamma < 0$, we have the KP-I case, and when $\alpha < 0$, $\gamma > 0$, $\beta > 0$, the KP-II case. The Kerr nonlinearity γ in Eq. (1) leads to a self-phase modulation of an optical pulse, and it transfers to the advection term in the hydrodynamic interpretation of Eq. (8).

Therefore, we underline that the optical NLSE solution $u(t, y, z)$ of hydrodynamic KP solution origin $[\eta(\tau, \upsilon, \varsigma), \phi(\tau, \upsilon, \varsigma)]$ with $\tau = t - c_0 z$, $\upsilon = y$, and $\varsigma = z$ can be written as:

$$u(t, y, z) = \sqrt{\rho_0 + \eta(\tau, \upsilon, \varsigma)}\, e^{i[\gamma\rho_0 z + \phi(\tau, \upsilon, \varsigma)]}. \tag{9}$$

In the following, we focus our attention on the anomalous dispersion and self-defocusing regime ($\alpha > 0$, $\beta > 0$, $\gamma < 0$), which leads to the KP-I case. The normal dispersion and self-focusing regime ($\alpha < 0$, $\gamma > 0$, $\beta > 0$), which leads to the KP-II case, will be analyzed in a future work. Without loss of generality, we set the following constraints to the coefficients of Eq. (1), $\alpha = 4\sqrt{2}$, $\beta = 6\sqrt{2}$, $\gamma = -2\sqrt{2}$; moreover, we fix $\rho_0 = 1$. Note that, with the previous relations among its coefficients, the Eq. (8) reduces to the standard KP-I form: $(-\eta_\varsigma - 6\eta\eta_\tau + \eta_{\tau\tau\tau})_\tau - 3\eta_{\upsilon\upsilon} = 0$.

Single NLSE dark lump solution of KP-I origin.—At first, we proceed to verify numerically the existence of $(2+1)$D NLSE dark-lump solitary waves, which is predicted by the KP-I through Eq. (9) (see, e.g., [18,27] for the lump solutions of KP-I). In our numerics, the input dark solitary wave envelope at $z = 0$ is given by the expression $u(t, y, 0) = \sqrt{1 + \eta(\tau, \upsilon, 0)}\exp[i\phi(\tau, \upsilon, 0)]$ with $\tau = t$ and $\upsilon = y$, where η is a bright lump solution of the KP-I Eq. (8), and $\phi_\tau = -(\gamma/c_0)\eta$.

When considering the small amplitude regime ($\epsilon \ll 1$), a form of KP lump-soliton solution of Eq. (8) can be

expressed as [27] $\eta(\tau,\upsilon,\varsigma) = -4[\epsilon^{-1} - (\tau - 3\epsilon\varsigma)^2 + \epsilon\upsilon^2]/[\epsilon^{-1} + (\tau - 3\epsilon\varsigma)^2 + \epsilon\upsilon^2]^2$. The parameter ϵ rules the amplitude, width, and velocity properties of the KP lump soliton. The lump peak amplitude in the (ς,υ) plane is -4ϵ; the velocity in the τ direction is 3ϵ. Moreover, $\phi(\tau,\upsilon,\varsigma) = 2\sqrt{2}\epsilon(\tau - 3\epsilon\varsigma)/[1 + \epsilon(\tau - 3\epsilon\varsigma) + \epsilon^2\upsilon^2]$.

Figure 1 shows the numerical spatiotemporal envelope intensity profile of a NLSE dark lump solitary wave in the y-t' plane ($t' = t - c_0 z$), at the input $z = 0$, and after the propagation distance $z = 100$, for $\epsilon = 0.05$. In the numerics, the initial dark NLSE profile of KP-I lump propagates stably in the z direction, with virtually negligible emission of dispersive waves, with the predicted velocity $c_0 + 3\epsilon$, and intensity dip of 4ϵ. Thus, the predicted theoretical dark lump solitary waves of Eq. (1) of the form (9) are well confirmed by numerical simulations.

Remarkably, our numerical studies have shown that the previously described NLSE–KP mapping works well also for values of ϵ which lead to strong perturbations of the stationary cw backgrounds (this will be reported elsewhere).

Elastic interaction of two single NLSE dark lumps.—Next, we consider the interaction of $(2+1)$D NLSE optical dark lumps based on the multilump solutions of the KP-I equation (see, e.g., [18,27,28]).

A formula for the exact multilump solution is available (see, e.g., [18,27,28]). However, when the lumps are well separated, a simple sum of those single lump solutions gives a good approximation of the exact N lump solution, that is, $\eta(\tau,\upsilon,\varsigma) \approx \sum_{i=1}^{N} -4[\epsilon_i^{-1} - (\tau_i - 3\epsilon_i\varsigma)^2 + \epsilon_i\upsilon_i^2]/[\epsilon_i^{-1} + (\tau_i - 3\epsilon_i\varsigma)^2 + \epsilon_i\upsilon_i^2]^2$, where ϵ_i rules the amplitude, width, and velocity properties of the i-lump soliton, $\tau_i = \tau - \tau_{0i}$, $\upsilon_i = \upsilon - \upsilon_{0i}$, define the i-lump's location.

Figure 2 shows the initial spatiotemporal envelope intensity profile $|u|^2$ of NLSE dark lumps for $N = 2$ in the y-t' plane along with the numerically computed profiles after propagation distances $z = 150$ and $z = 300$. Here, $\epsilon_1 = 0.09$, $\tau_{01} = -20$, $\upsilon_{01} = 0$, $\epsilon_2 = 0.01$, $\tau_{02} = 0$, $\upsilon_{02} = 0$. One can see from Fig. 2 that two dark lumps with different amplitudes show an *elastic* interaction: the tall lump approaches the small one along the t' axis, then they interact and generate a waveform with two separate peaks in the y direction. After the interaction, the tall soliton is in front of the small one, and those lumps keep their profiles.

Abnormal scattering of NLSE dark lump solution.—At last, we remark that the KP-I equation admits another class of lump solutions which have several peaks with the same amplitude in the asymptotic stages $|z| \gg 0$ (see, e.g., [29,30]). Following [30], we call such lump solution *multipole lump*. Here, we demonstrate that the $(2+1)$D NLSE can also support such lump solution. We consider a

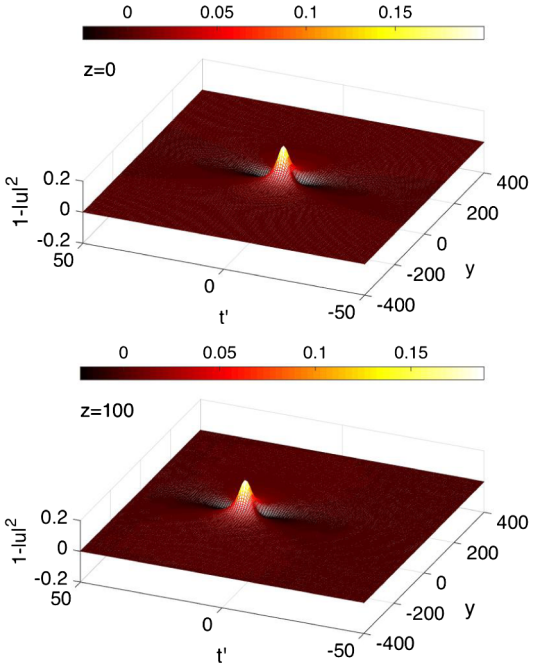

FIG. 1. Numerical spatiotemporal dark-lump NLSE envelope intensity distribution $1 - |u|^2$, shown in the y-t' plane with $t' = t - c_0 z$, at $z = 0$, and $z = 100$. Here, $\epsilon = 0.05$.

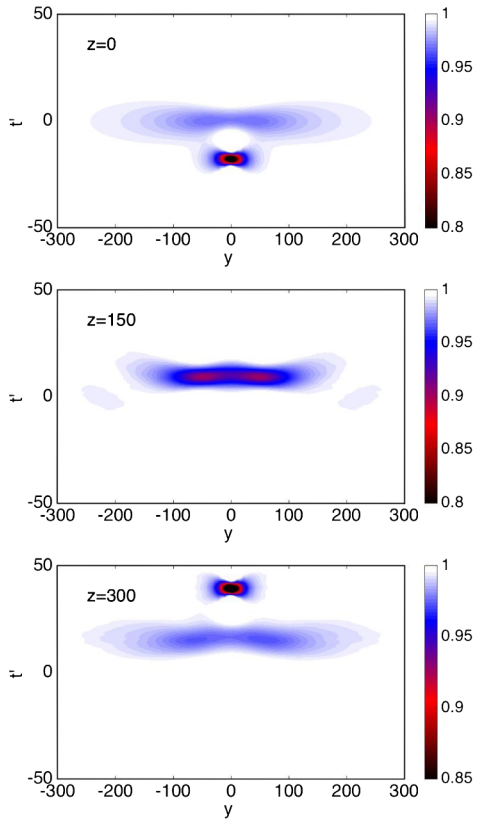

FIG. 2. Numerical spatiotemporal NLSE envelope intensity distribution $|u|^2$, in the y-t' plane, showing the interaction of two dark lumps ($N = 2$), at the input $z = 0$, at $z = 150$, and $z = 300$. Here, $\epsilon_1 = 0.09$, $\tau_{01} = -20$, $\upsilon_{01} = 0$, $\epsilon_2 = 0.01$, $\tau_{02} = 0$, $\upsilon_{02} = 0$.

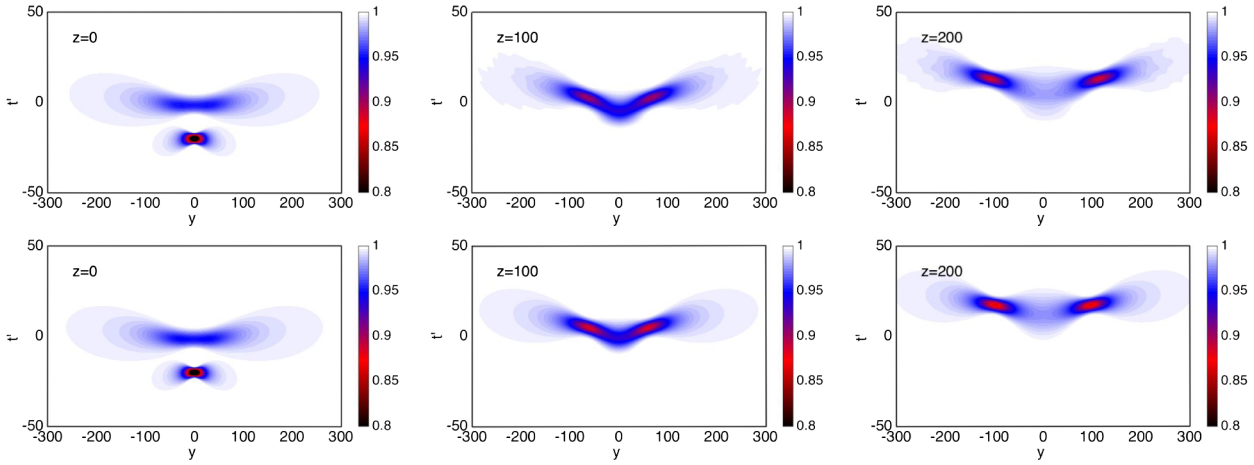

FIG. 3. Spatiotemporal NLSE envelope intensity distribution $|u|^2$, in the y-t' plane, showing anomalous scattering of dark waves, at $z = 0$, at $z = 100$, and $z = 200$. Top, numerical simulations; bottom theoretical prediction Eq. (9) with KP-I multipole lump solution. Here, $\epsilon = 0.1$, $\tau_0 = 0$, $\upsilon_0 = 0$, $\varsigma_0 = -50$, $\delta_1 = 0$, $\delta_2 = 0$.

multipole lump solution with two peaks, which is expressed as [30]: $\eta(\tau, \upsilon, \varsigma) = -2\partial_\tau^2 \log F$, where $F = |f_1^2 + if_2 + f_1/\epsilon + 1/2\epsilon^2|^2 + |f_1 + 1/\epsilon|^2/2\epsilon^2 + 1/4\epsilon^4$, and $f_1 = \tau_1 + 2i\epsilon\upsilon_1 - 12\epsilon^2\varsigma_1 + \delta_1$, $f_2 = -2\upsilon - 24i\epsilon\varsigma + \delta_2$. $\tau_1 = \tau - \tau_0$, $\upsilon_1 = \upsilon - \upsilon_0$, $\varsigma_1 = \varsigma - \varsigma_0$ define the dislocation; δ_1, δ_2 are arbitrary complex parameters.

Figure 3 (top) shows the initial spatiotemporal envelope intensity profile $|u|^2$ of a two peaked NLSE dark lump in the y-t' plane, along with the numerically computed profiles after propagation distances $z = 100$ and $z = 200$, for $\epsilon = 0.1$ ($\tau_0 = 0$, $\upsilon_0 = 0$, $\varsigma_0 = -50$, $\delta_1 = 0$, $\delta_2 = 0$). In particular, Fig. 3 depicts the scattering interaction of the two-peaked waves: two dark lumps approach each other along the t' axis, interact, and recede along the y axis. These solutions exhibit anomalous (nonzero deflection angles) scattering due to multipole structure in the wave function of the inverse scattering problem. We remark that the numerical result of NLSE dynamics is in very good agreement with the analytical dark solitary solution Eq. (9) with a KP-I multipole lump solution, as seen in Fig. 3 (bottom). Only weak discrepancies are visible in the wings of the double lumps, owing to dispersive waves generated during the collision, as a result of higher order effects to the KP approximation.

Experiments in Optics.—Let us briefly discuss a possible experimental setting in nonlinear optics for the observation of cubic spatiotemporal solitary wave dynamics of hydrodynamic origin. As to $(2+1)$D spatiotemporal dynamics, one may consider optical propagation in a planar glass waveguide (e.g., see the experimental setup of Ref. [9]), or a quadratic lithium niobate planar waveguide, in the regime of high phase mismatch, which mimics an effective Kerr nonlinear regime (e.g., see the experimental setup of Ref. [11]). As to $(2+1)$D spatial dynamics, one may consider a cw Ti:sapphire laser and a nonlinear medium composed of atomic-rubidium vapor (e.g., see the experimental setup of Ref. [24]) or a bulk quadratic lithium niobate crystal, in the regime of high phase-mismatch (e.g., see the experimental setup of Refs. [12,31]).

The excitation of spatiotemporal dark lump solitary waves from nonideal input conditions is a relevant problem for the experiments, and it will be the subject of further investigations.

As a final remark, note that the well-known modulation instability (MI) of plane waves [13,32] or conical emission, in general, may emerge in the $(2+1)$D NLSE scenario. In the case we have considered, that is anomalous dispersion and self-defocusing regime ($\alpha > 0$, $\beta > 0$, $\gamma < 0$, the NLSE- KP-I correspondence), MI is absent. Thus, the lumps' evolution does not suffer the presence of noise. On the other hand, when considering the normal dispersion and self-focusing regime ($\alpha < 0$, $\gamma > 0$, $\beta > 0$, the NLSE—KP-II correspondence) MI plays a crucial competing role. In fact, the modulation instability of the cw background may compete and ultimately spoil, for sufficiently long propagation distances, the propagation and interaction of dark solitary waves in $(2+1)$D NLSE propagation.

Conclusions.—We have analytically predicted a new class of dark solitary wave solutions that describe nondiffractive and nondispersive spatiotemporal localized wave packets propagating in optical Kerr media. We numerically confirmed the existence, stability, and peculiar elastic and anomalous scattering interactions of dark-lump solitary waves of the $(2+1)$D NLSE. The key novel property of these solutions is that their existence and interactions are inherited from the hydrodynamic soliton solutions of the well-known KP equation. Our findings open a new avenue for research in spatiotemporal extreme nonlinear optics. Given that deterministic optical rogue and shock wave solutions, so far, have been essentially restricted to $(1+1)$D models [33–39], multidimensional spatiotemporal nonlinear waves would lead to a

substantial qualitative enrichment of the landscape of extreme wave phenomena.

The present research was supported by the Italian Ministry of University and Research (MIUR, Project No. 2012BFNWZ2). The research of Y. K. is partially supported by NSF Grant No. DMS-1410267.

*fabio.baronio@unibs.it
†kodama@math.ohio-state.edu

[1] R. Boyd, *Nonlinear Optics* 3rd ed (Academic Press, London, 2008).
[2] Y. Silberberg, Opt. Lett. **15**, 1282 (1990).
[3] J. E. Rothenberg, Opt. Lett. **17**, 583 (1992).
[4] J. K. Ranka, R. W. Schirmer, and A. L. Gaeta, Phys. Rev. Lett. **77**, 3783 (1996).
[5] J. R. Ranka and A. L. Gaeta, Opt. Lett. **23**, 534 (1998).
[6] A. A. Zozulya, S. A. Diddams, A. G. Van Engen, and T. S. Clement, Phys. Rev. Lett. **82**, 1430 (1999).
[7] X. Liu, L. J. Qian, and F. W. Wise, Phys. Rev. Lett. **82**, 4631 (1999).
[8] I. G. Koprinkov, A. Suda, P. Wang, and K. Midorikawa, Phys. Rev. Lett. **84**, 3847 (2000).
[9] H. S. Eisenberg, R. Morandotti, Y. Silberberg, S. Bar-Ad, D. Ross, and J. S. Aitchison, Phys. Rev. Lett. **87**, 043902 (2001).
[10] S. Tzortzakis, L. Sudrie, M. Franco, B. Prade, and M. Mysyrowicz, A. Couairon, and L. Bergé, Phys. Rev. Lett. **87**, 213902 (2001).
[11] P. H. Pioger, V. Couderc, L. Lefort, A. Barthelemy, F. Baronio, C. De Angelis, Y. Min, V. Quiring, and W. Sohler, Opt. Lett. **27**, 2182 (2002).
[12] F. Baronio, C. De Angelis, P. H. Pioger, V. Couderc, and A. Barthelemy, Opt. Lett. **29**, 986 (2004).
[13] C. Conti, S. Trillo, P. Di Trapani, G. Valiulis, A. Piskarskas, O. Jedrkiewicz, and J. Trull, Phys. Rev. Lett. **90**, 170406 (2003).
[14] P. Di Trapani, G. Valiulis, A. Piskarskas, O. Jedrkiewicz, J. Trull, C. Conti, and S. Trillo, Phys. Rev. Lett. **91**, 093904 (2003).
[15] O. Jedrkiewicz, A. Picozzi, M. Clerici, D. Faccio, and P. Di Trapani, Phys. Rev. Lett. **97**, 243903 (2006).
[16] B. B. Kadomtsev and V. I. Petviashvili, Sov. Phys. Dokl. **15**, 539 (1970).
[17] J. Miles, J. Fluid Mech. **79**, 157 (1977); **79**, 171 (1977).
[18] M. J. Ablowitz and H. Segur, *Solitons and the Inverse Scattering Transform*, SIAM Studies in Applied Mathematics (SIAM, Philadelphia, 1981).
[19] Y. Kodama, J. Phys. A **43**, 434004 (2010).
[20] W. Li, H. Yeh, and Y. Kodama, J. Fluid Mech. **672**, 326 (2011).
[21] E. A. Kuznetsov and S. K. Turitsyn, Sov. Phys. JEPT **67**, 1583 (1988).
[22] G. A. Swartzlander and C. T. Law, Phys. Rev. Lett. **69**, 2503 (1992).
[23] D. E. Pelinovsky, Y. A. Stepanyants, and Y. S. Kivshar, Phys. Rev. E **51**, 5016 (1995).
[24] V. Tikhonenko, J. Christou, B. Luther-Davies, and Y. S. Kivshar, Opt. Lett. **21**, 1129 (1996).
[25] D. J. Frantzeskakis, K. Hizanidis, B. A. Malomed, and C. Polymilis, Phys. Lett. A **248**, 203 (1998).
[26] Y. Kodama and S. Wabnitz, Opt. Lett. **20**, 2291 (1995).
[27] S. V. Manakov, V. E. Zakharov, L. A. Bordag, and V. B. Matveev, Phys. Lett. **63A**, 205 (1977).
[28] Z. Lu, E. M. Tian, and R. Grimshaw, Wave Motion **40**, 123 (2004).
[29] R. S. Johnson and S. Thompson, Phys. Lett. **66A**, 279 (1978).
[30] M. J. Ablowitz, S. Chakravarty, A. D. Trubatch, and J. Villarroel, Phys. Lett. A **267**, 132 (2000).
[31] K. Krupa, A. Labruyre, A. Tonello, B. M. Shalaby, V. Couderc, F. Baronio, and A. B. Aceves, Optica **2**, 1058 (2015).
[32] A. G. Litvak and V. I. Talanov, Radiophys. Quantum Electron. **10**, 296 (1967); H. C. Yuen and B. M. Lake, Annu. Rev. Fluid Mech. **12**, 303 (1980); P. K. Newton and J. B. Keller, SIAM J. Appl. Math. **47**, 959 (1987).
[33] B. Kibler, J. Fatome, C. Finot, G. Millot, F. Dias, G. Genty, N. Akhmediev, and J. M. Dudley, Nat. Phys. **6**, 790 (2010).
[34] F. Baronio, A. Degasperis, M. Conforti, and S. Wabnitz, Phys. Rev. Lett. **109**, 044102 (2012).
[35] M. Onorato, S. Residori, U. Bortolozzo, A. Montina, and F. T. Arecchi, Phys. Rep. **528**, 47 (2013).
[36] F. Baronio, M. Conforti, A. Degasperis, S. Lombardo, M. Onorato, and S. Wabnitz, Phys. Rev. Lett. **113**, 034101 (2014).
[37] S. Randoux, P. Walczak, M. Onorato, and P. Suret, Phys. Rev. Lett. **113**, 113902 (2014).
[38] M. Conforti, F. Baronio, and S. Trillo, Phys. Rev. A **89**, 013807 (2014).
[39] B. Kibler, A. Chabchoub, A. Gelash, N. Akhmediev, and V. E. Zakharov, Phys. Rev. X **5**, 041026 (2015).